Modal Analysis of Conical Shell Filled with Fluid

Myung Jo Jhung*, **Jong Chull Jo**
Korea Institute of Nuclear Safety,
19 Guseong-dong, Yuseong-gu, Daejeon 305-338, Korea
Kyeong Hoon Jeong
Korea Atomic Energy Research Institute,
150 Dukjin-dong, Yuseong-gu, Daejeon 305-353, Korea

As a basic study on the fluid-structure interaction of the shell structure, a theoretical formulation has been suggested on the free vibration of a thin-walled conical frustum shell filled with an ideal fluid, where the shell is assumed to be fixed at both ends. The motion of fluid coupled with the shell is determined by means of the velocity potential flow theory. In order to calculate the normalized natural frequencies that represent the fluid effect on a fluid-coupled system, finite element analyses for a fluid-filled conical frustum shell are carried out. Also, the effect of apex angle on the frequencies is investigated.

Key Words : Conical Shell, Modal Characteristic, Finite Element Method, Apex Angle

1. Introduction

A thin conical frustum shell filled with fluid is widely used in the engineering design. One example is a support shell bounded by top and bottom rigid plates in an integral reactor that is under development in Korea. The support shell is a perforated conical frustum shell in contact with coolant during the power plant operation. To verify the structural integrity during normal operation, it is necessary to investigate extensively flow induced vibration, prerequisite to which is the investigation of the modal characteristics.

The basic studies on the modal analysis of a conical frustum shell in vacuum have been performed by Goldburg et al. (1960). However, few theoretical studies on free vibration of a conical frustum shell filled with fluid were taken into consideration. Instead of the conical shell, many researchers have studied similar problems, both theoretically and experimentally. Yamaki et al. (1984) and Gupta et al. (1988) developed an analytical method for free vibration of a clamped cylindrical shell filled with an ideal fluid using the Galerkin procedure. An experimental study was carried out and verified with FEM by Mazuch et al. (1996). Han and Liu (1994) considered tanks with axial non-uniformity in the thickness when studying the same problem. Jeong and Kim (1998) also developed a theoretical method for the free vibration of a circular cylindrical shell filled with a compressible bounded fluid using Fourier series expansion method. Jeong et al. (1997) investigated the effects of compressibility of fluid and fluid density on the coupled natural frequencies of a cylindrical tank filled with compressible fluid.

This study attempts to suggest an analytical approach that can calculate the natural frequencies of a conical frustum shell filled with a bounded ideal fluid. The fixed boundary condition is assumed for both ends of the shell. An example to predict the natural frequencies of a conical shell filled with an inviscous and incompressible fluid is predicted using finite element analysis in order to investigate fluid effect on free vibration of the

* Corresponding Author,
E-mail : mjj@kins.re.kr
TEL : +82-42-868-0467; **FAX** : +82-42-861-9945
Korea Institute of Nuclear Safety, 19 Guseong-dong, Yuseong-gu, Daejeon 305-338, Korea. (Manuscript **Received** January 6, 2006; **Revised** August 23, 2006)

fluid-filled conical shell. Also investigated in this study is the effect of apex angle on the frequencies of the conical shell.

2. Theory

2.1 Equation of motion

Consider a conical frustum shell containing incompressible fluid covered by rigid end plates, as illustrated in Fig. 1. The shell has an upper radius R_2, lower radius R_1, height H, and wall thickness h. The Donnell-Mushtari's shell equations (Leissa, 1973) coupled with a fluid effect can be written as:

$$\left[\frac{\partial^2 u}{\partial \tilde{s}^2}+\sin\alpha\frac{\partial u}{\partial \tilde{s}}+\left(\frac{1-\mu}{2}\right)\frac{\partial^2 u}{\partial\theta^2}-(\sin^2\alpha)\,u\right]+\left[\left(\frac{1+\mu}{2}\right)\frac{\partial^2 v}{\partial\tilde{s}\partial\theta}-\left(\frac{3-\mu}{2}\right)\sin\alpha\frac{\partial v}{\partial\theta}\right]+\cos\alpha\left[\mu\frac{\partial w}{\partial\tilde{s}}-\sin\alpha\, w\right]=\frac{\rho(1-\mu^2)R_o^2}{E}\frac{\partial^2 u}{\partial t^2} \tag{1a}$$

$$\left[\left(\frac{1+\mu}{2}\right)\frac{\partial^2 u}{\partial\tilde{s}\partial\theta}+\left(\frac{3-\mu}{2}\right)\sin\alpha\frac{\partial u}{\partial\theta}\right]+\left(\frac{1-\mu}{2}\right)\left[\frac{\partial^2 v}{\partial\tilde{s}^2}+\sin\alpha\frac{\partial v}{\partial\tilde{s}}-\sin^2\alpha\, v\right]+\frac{\partial^2 v}{\partial\theta^2}+\left[\cos\alpha\frac{\partial w}{\partial\theta}\right]=\frac{\rho(1-\mu^2)R_o^2}{E}\frac{\partial^2 v}{\partial t^2} \tag{1b}$$

$$\cos\alpha\left[\mu\frac{\partial u}{\partial\tilde{s}}+\sin\alpha\, u\right]+\left[\cos\alpha\frac{\partial v}{\partial\theta}\right]+\left[\cos^2\alpha\, w+\frac{h^2}{12R_o^2}\nabla^4 w\right]=-\frac{\rho(1-\mu^2)R_o^2}{E}\frac{\partial^2 w}{\partial t^2}-\frac{p(1-\mu^2)R_o^2}{Eh} \tag{1c}$$

where, $\tilde{s}=s/R_o$, α=apex angle of the shell, ρ= mass density of the shell, μ=Poisson's ratio of the shell, p=hydro-dynamic pressure on the shell, E=modulus of elasticity and u, v and w are modal functions of the shell corresponding to the s, θ and r directions, respectively. The biharmonic operator can be defined as the particular coordinates.

$$\nabla^4=\left[\frac{\partial^2}{\partial\tilde{s}^2}+\sin\alpha\frac{\partial}{\partial\tilde{s}}+\frac{\partial^2}{\partial\theta^2}\right]^2 \tag{2}$$

When the shell is simply supported at the both

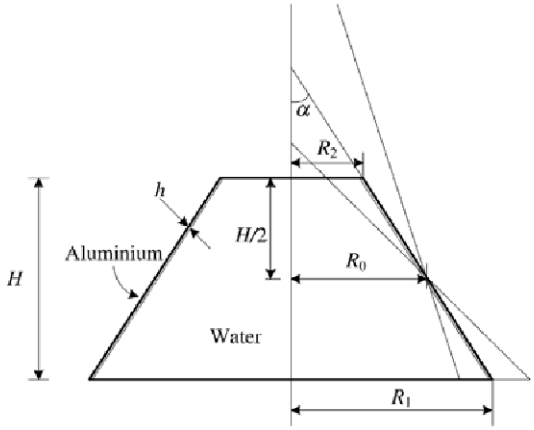

Fig. 1 A conical shell filled with fluid

ends, the boundary conditions are at $s=0$ and $s=L$:

$$M_s(0)=N_s(0)=v(0)=w(0)=M_s(L)=N_s(L)=v(L)=w(L)=0 \tag{3a}$$

where N_S and M_S denote the membrane tensile force and bending moment per unit length, respectively. On the other hand, when the shell is fixed at the both ends, the geometric boundary conditions of the shell are at $s=0$ and $s=L$:

$$u(0)=v(0)=w(0)=w_{,s}(0)=u(L)=v(L)=w(L)=w_{,s}(L)=0 \tag{3b}$$

2.2 Modal functions

When the conical frustum shell is simply supported or fixed at both ends, the dynamic displacements in any mode of free vibration can be assumed in the following form for any circumferential mode number n:

$$u(s,\theta,t)=\sum_{m=1}^{8}[A_{nm}\exp\{\lambda_{nm}(\tilde{s}-\tilde{s}_1)\}]\cos n\theta\exp(i\omega t) \tag{4a}$$

$$v(s,\theta,t)=\sum_{m=1}^{8}[B_{nm}\exp\{\lambda_{nm}(\tilde{s}-\tilde{s}_1)\}]\sin n\theta\exp(i\omega t) \tag{4b}$$

$$w(s,\theta,t)=\sum_{m=1}^{8}[C_{nm}\exp\{\lambda_{nm}(\tilde{s}-\tilde{s}_1)\}]\cos n\theta\exp(i\omega t) \tag{4c}$$

where $\tilde{s}_1=s_1/R_o$. A_{nm}, B_{nm} and C_{nm} in Eq. (4) denote the unspecified coefficients that define the mode shapes of the shell and depend on the chosen boundary conditions. λ_{nm} in Eq. (4) is the frequency parameter.

2.3 Equation of fluid motion

The contained fluid does not maintain a free surface since it is bounded by the rigid end plates at both ends of the shell. The non-viscous, irrotational and incompressible fluid motion due to the shell vibration is described by the general velocity potential Φ which must satisfy the Laplace equation :

$$\Phi_{,RR}+\frac{1}{R}\Phi_{,R}+\frac{1}{R^2}\Phi_{,\theta\theta}+\Phi_{,xx}=0 \quad (5)$$

It is possible to separate the function Φ with respect to x by observing that the rigid plates attached to both ends of the shell prevent the fluid from moving to the x direction. The solution can be obtained with respect to the cylindrical coordinates, R, θ and x.

$$\begin{aligned}\Phi(R,\theta,x,t)&=\phi(R,\theta,x)\exp(i\omega t)\\&=\sum_{m=1}^{8}D_{nm}I_n(\lambda_{nm}\tilde{R})\cos(\lambda_{nm}\tilde{x})\cos n\theta\exp(i\omega t)\end{aligned} \quad (6)$$

where $\tilde{R}=R/R_o$, $\tilde{x}=x/R_o$, and ω is the coupled natural frequency of the shell. I_n is modified Bessel function of the first kind of order n. ϕ means the spatial velocity potential of the contained fluid. Because of impermeable rigid surface on the bottom and the top, the axial fluid velocity there is also zero, so at $x=0$ and $x=H$

$$\partial\phi(R,\theta,x)/\partial x=0 \quad (7)$$

In addition, when the thickness of the shell is negligible compared to the shell diameter, the boundary condition assures the contact between the inner surface of the shell and the fluid. The requirement is given as at $R=R_0$:

$$\begin{aligned}\partial\phi(R,\theta,x)/\partial r&=\partial\phi(R,\theta,x)\cos\alpha/\partial R\\&=-w(s,\theta)\end{aligned} \quad (8)$$

From Eq. (8), the unspecified coefficient D_{nm} in Eq. (6), associated with the fluid motion, can be described in terms of the modal coefficient C_{nm} associated with the radial displacement of the shell ;

$$\begin{aligned}&\lambda_{nm}D_{nm}I_n'(\lambda_{nm})\cos\alpha\cos(\lambda_{nm}\tilde{x})\\&=-C_{nm}\cos\{\lambda_{nm}(\tilde{s}-\tilde{s}_1)\}\end{aligned} \quad (9)$$

Further, the hydrodynamic pressure exerted by the fluid on the wetted shell surface can be given as ;

$$p(x,\theta,t)=\rho_o\omega^2\phi(R_o,\theta,\tilde{x})\exp(i\omega t) \quad (10)$$

where ρ_o is the fluid density. Now, the normalized forces due to the hydrodynamic pressure on the wetted shell surface, namely $p(1-\mu^2)R_o^2/Eh$, in Eq. (1c), can be reduced in terms of coefficient C_{nm} associated with the radial displacement of the conical shell :

$$\begin{aligned}&\frac{p(1-\mu^2)R_o^2}{Eh}\\&=-\frac{\rho_o\omega^2(1-\mu^2)R_o^2}{Eh}\sum_{m=1}^{8}C_{nm}\Lambda_{nm}\cos\{\lambda_{nm}(\tilde{s}-\tilde{s}_1)\}\cos n\theta\exp(i\omega t)\end{aligned} \quad (11)$$

where

$$\Lambda_{nm}=-I_n(\lambda_{nm})/(\lambda_{nm}I_n'(\lambda_{nm})\cos\alpha) \quad (12)$$

2.4 General formulation

Substitution of the displacements described by Eq. (4) and Eq. (11) into Eq. (1), leads to an explicit relation for the coefficients A_{nm}, B_{nm} and C_{nm} which are coupled together as follows :

$$\begin{bmatrix}e_{11}&e_{12}&e_{13}\\e_{12}&e_{22}&e_{23}\\e_{13}&e_{23}&e_{33}\end{bmatrix}\begin{Bmatrix}A_{nm}\\B_{nm}\\C_{nm}\end{Bmatrix}=[\mathbf{S}]\begin{Bmatrix}A_{nm}\\B_{nm}\\C_{nm}\end{Bmatrix}=\{0\} \quad (13)$$

The elements of the matrix, e_{ij} $(i,j=1,2,3)$ can be obtained from formulation of Eq. (13). For a non-trivial solution of Eq. (13), the determinant of the matrix, det$[\mathbf{S}]$ must vanish.

$$|\mathbf{S}|=0 \quad (14)$$

This requirement gives a characteristic equation which leads to an algebraic equation of the eighth order for the unknown eigenvalues, λ_{nm}. Eq. (13) also allows us to calculate the ratios of the coefficients A_{nm}/C_{nm} and B_{nm}/C_{nm}. The global solution will thus be given with the help of eight integration coefficients and unknown frequency parameter. The final phase of the calculation procedure lies in satisfying the corresponding boundary condtions described by Eqs. (3a) and (3b). Since four boundary conditions are to be satisfied at each shell edge, we obtain a total of eight conditions to be satisfied by solving Eq. (4). This produces 8 linear homogeneous equations for eight integration coefficients, for each value of n. The condition requiring that these integration coefficients be zero leads to the frequency determinant.

3. Analysis

3.1 Theoretical analysis

On the basis of the preceding analysis, the frequency determinant is numerically solved for the clamped boundary condition in order to find the natural frequencies of a conical shell filled with fluid. The shell has a mean radius of 150 mm at mid-height, a length of 300 mm, and a wall thickness of 2 mm. The physical properties of the shell material are as follows: Young's modulus=69.0 GPa, Poisson's ratio=0.3, and mass density=2700 kg/m^3. Water is used as the contained fluid with a density of 1000 kg/m^3. The sound speed in water, 1483 m/s, is equivalent to the bulk modulus of elasticity, 2.2 GPa.

The frequency equation derived in the preceding section involves the double infinite series of algebraic terms. Before exploring the analytical method for obtaining the natural frequencies, it is necessary to conduct convergence studies and establish the number of terms required in the series expansions involved. In the numerical calculation, the Fourier expansion term is set at 100, which gives an exact enough solution by convergence

3.2 Finite element analysis

Finite element analyses using a commercial com-

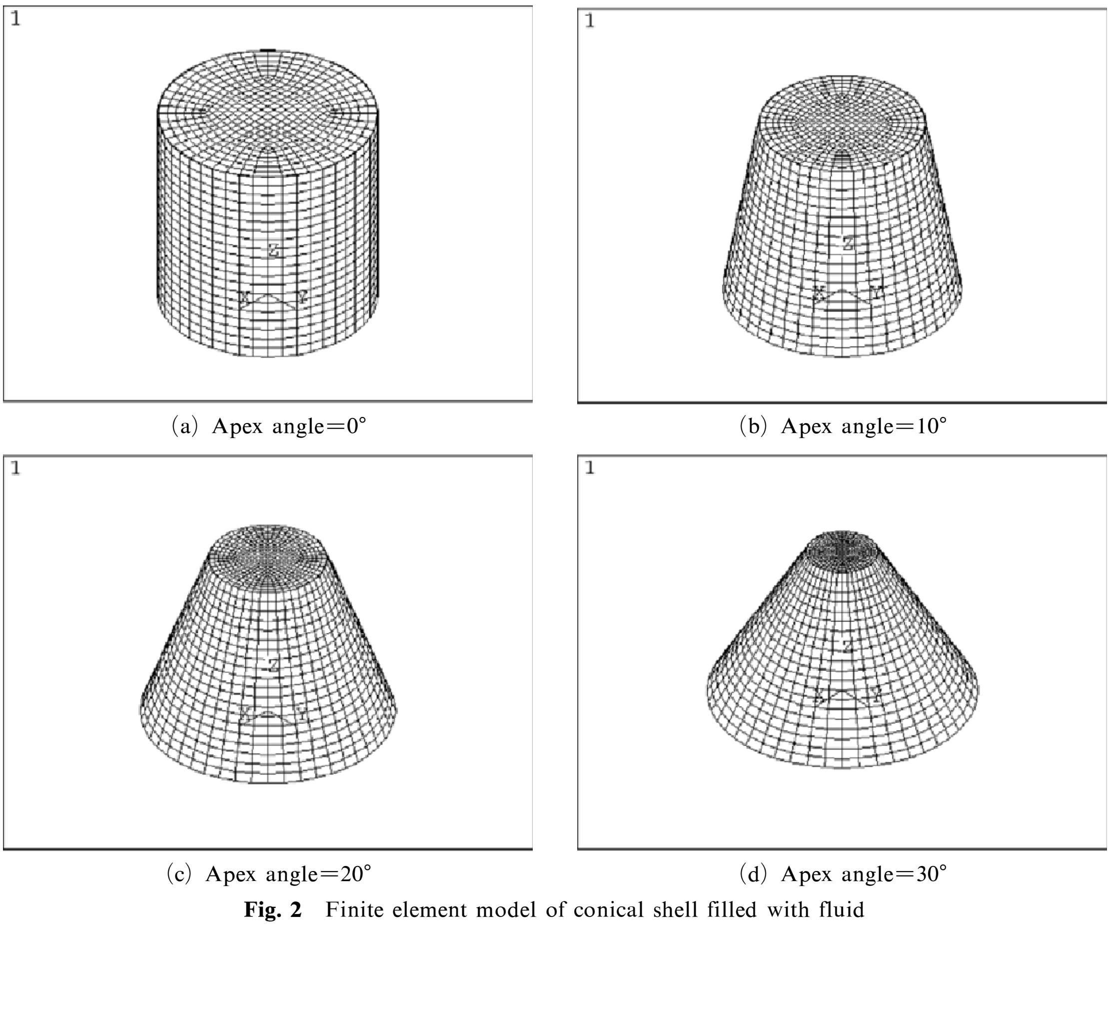

(a) Apex angle=0° (b) Apex angle=10°

(c) Apex angle=20° (d) Apex angle=30°

Fig. 2 Finite element model of conical shell filled with fluid puter code ANSYS 5.6 (ANSYS, 1999) are performed to verify the analytical results for the theoretical study. The finite element method results are used as the baseline data. Three-dimensional model is constructed for the finite element analysis. The fluid region is divided into a number of identical 3-dimensional contained fluid elements (FLUID80) with eight nodes having three degrees of freedom at each node. The fluid element FLUID80 is particularly well suited for calculating hydrostatic pressures and fluid/solid interactions. The circular cylindrical shell is modeled as elastic shell elements (SHELL63) with four nodes. The model has 8640 fluid elements and 960 shell elements as shown in Fig. 2.

The fluid boundary conditions at the top and bottom of the tank are zero displacement and rotation. The nodes connected entirely by the fluid elements are free to move arbitrarily in three-dimensional space, with the exception of those, which are restricted to motion in the bottom and top surfaces of the fluid cavity. The radial velocities of the fluid nodes along the wetted shell surfaces coincide with the corresponding velocities

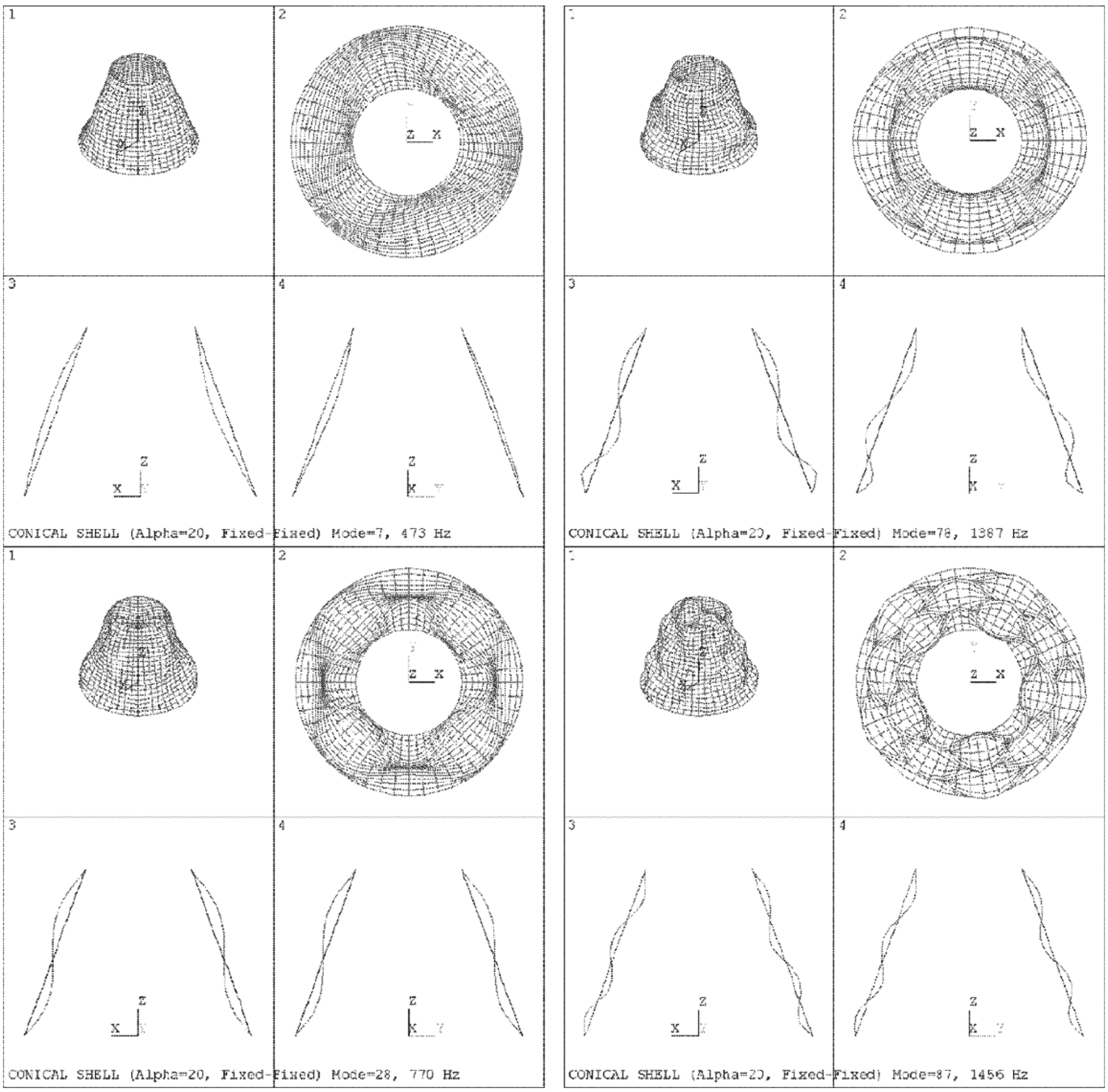

Fig. 3 Typical mode shapes of conical shell with fluid for $\alpha=20°$

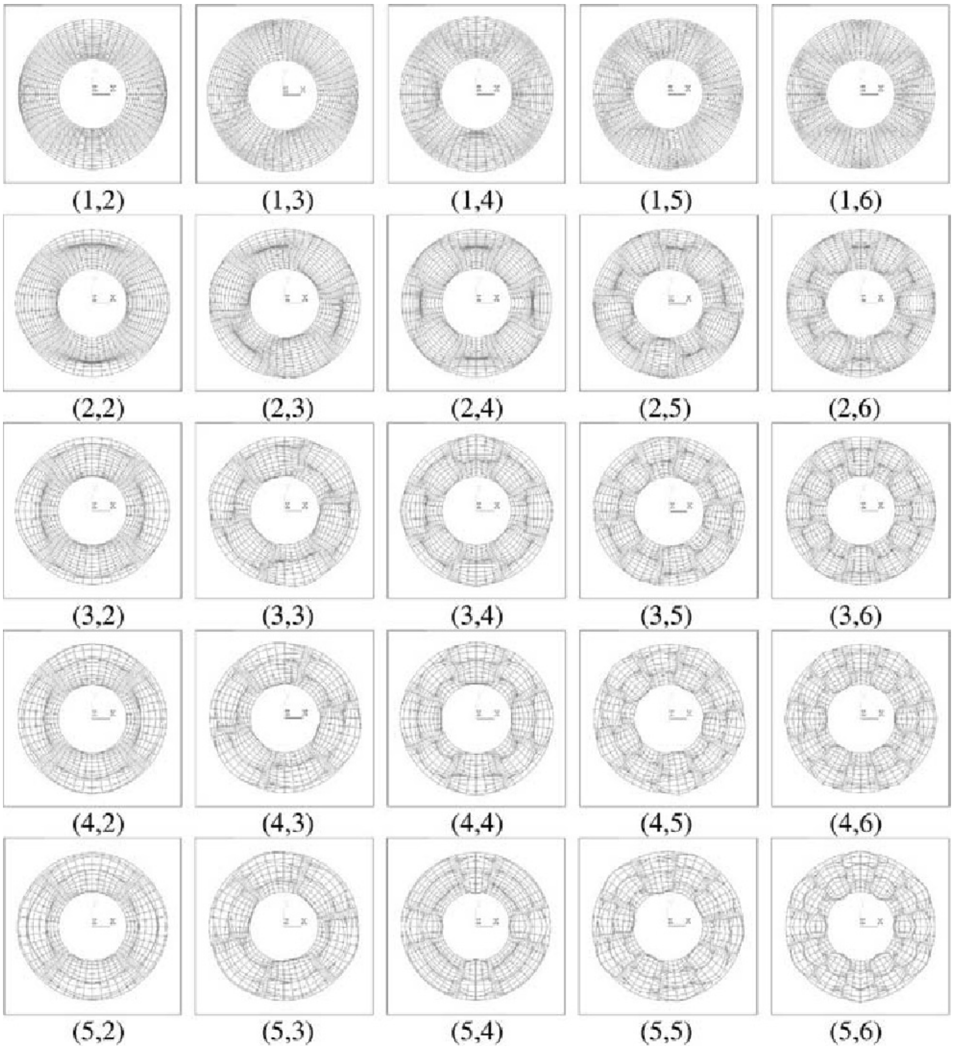

Fig. 4 Mode shapes of conical shell with fluid for $\alpha=20°$

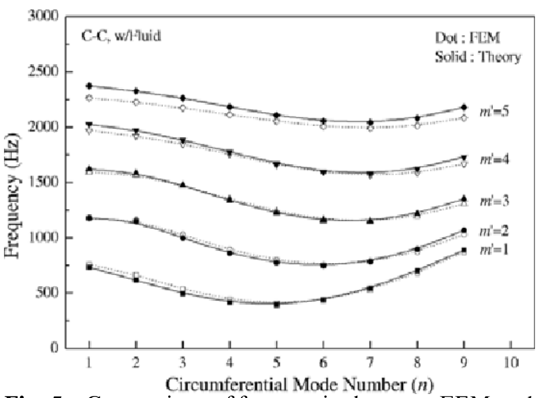

Fig. 5 Comparison of frequencies between FEM and theory for a conical shell with fluid

of the shells. Clamped-clamped boundary conditions at both ends are considered for the shell.

The Block Lanczos method is used for the eigenvalue and eigenvector extractions of the finite element model, which is available for large symmetric eigenvalue problem. Typically this solver is applicable to the type of problems solved using the subspace eigenvalue method, however, at a faster convergence rate, and is very useful to find all exact symmetric modes necessary to define the dynamic characteristics of the shell. In this case several sloshing modes of a fluid appear at the same time and therefore they should be excluded for the shell modes only.

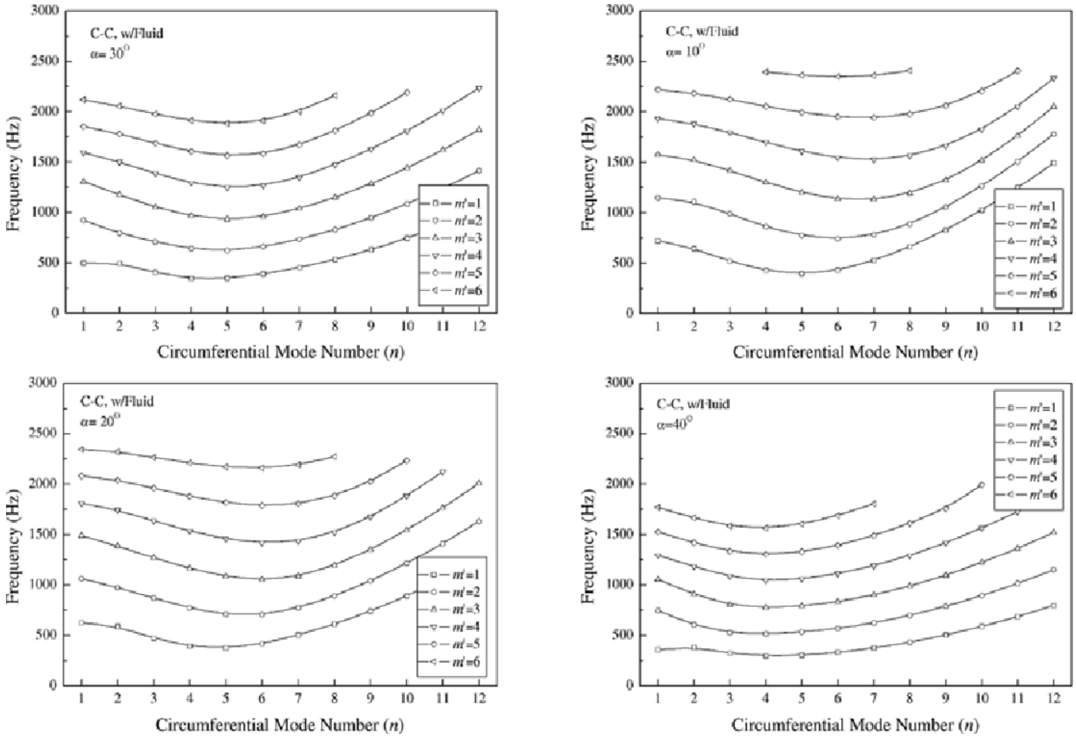

Fig. 6 Natural frequencies of a conical shell with fluid

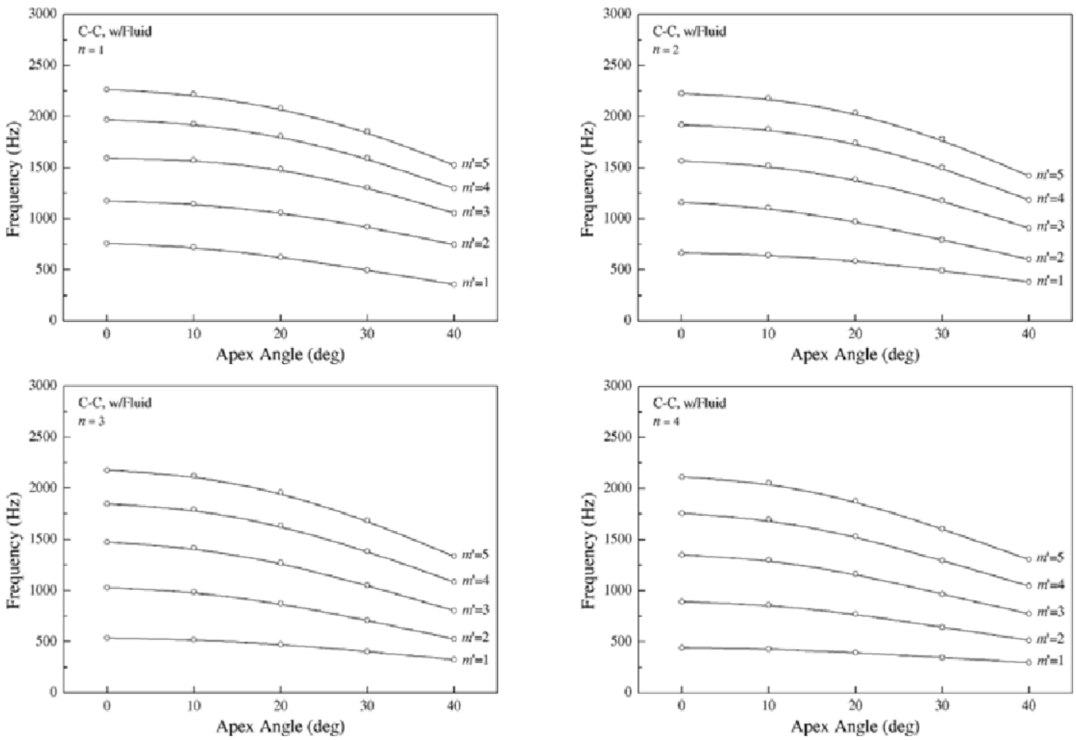

Fig. 7 Frequency comparisons of a conical shell with fluid

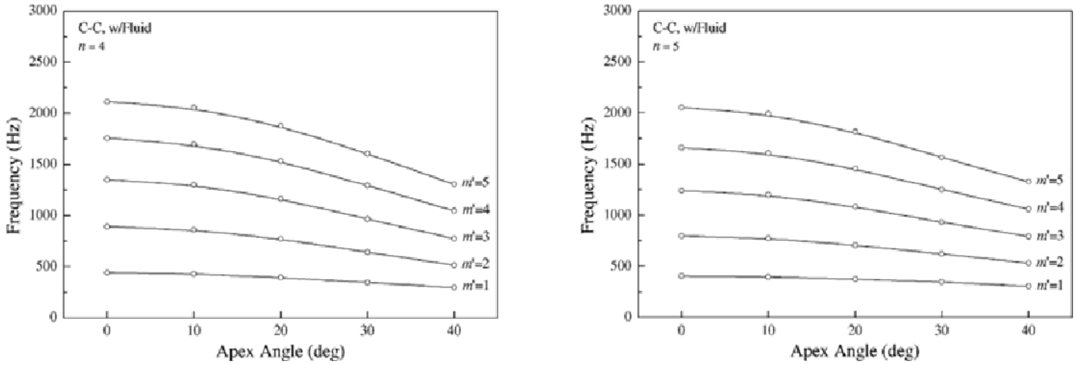

Fig. 7 Frequency comparisons of a conical shell with fluid (Cont'd)

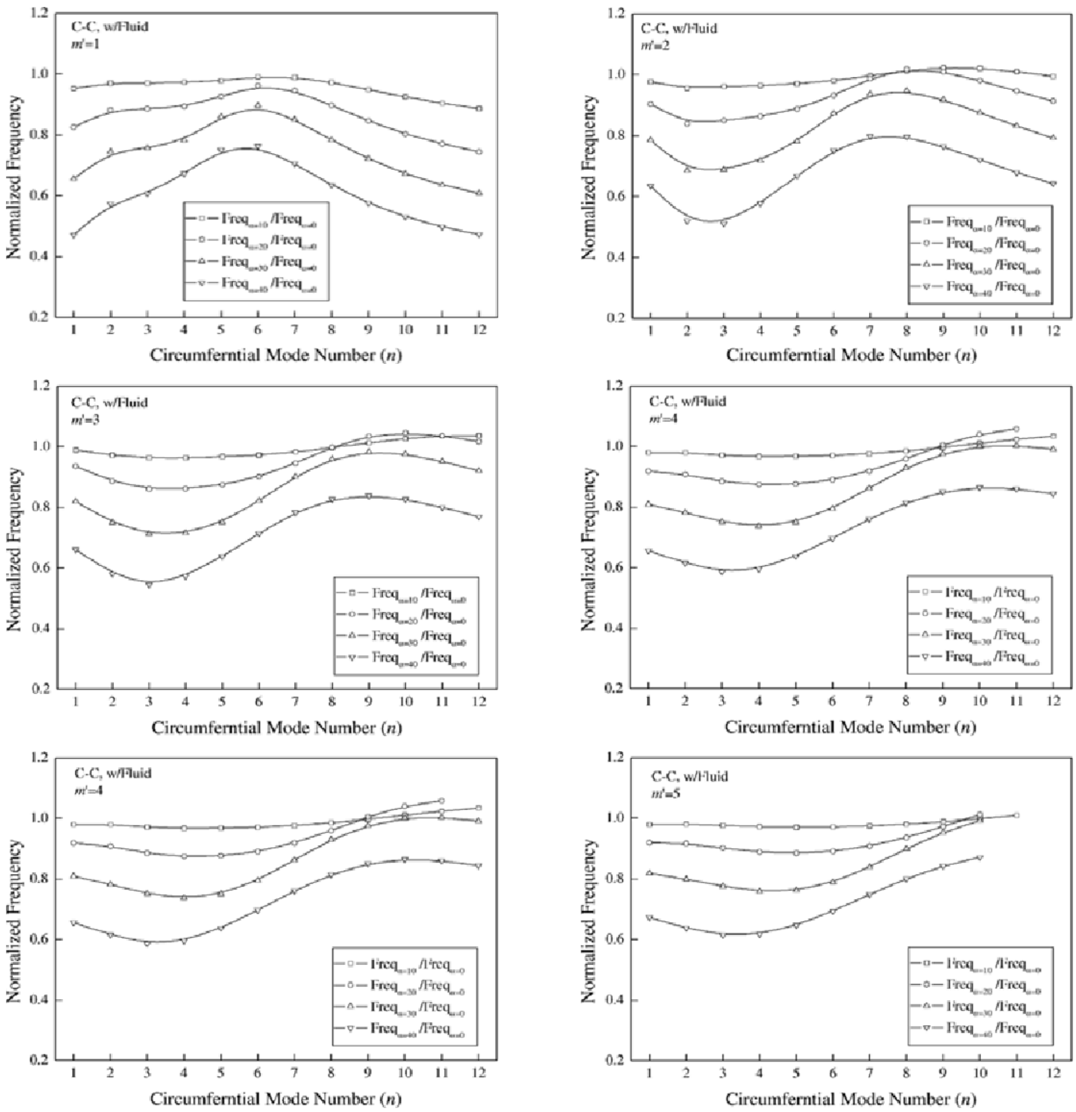

Fig. 8 Normalized frequencies of a conical shell to cylindrical shell

4. Results and Discussion

Mode shapes of a conical shell are obtained by the finite element method and typical modes are plotted in Fig. 3, which shows the deformed mode shape of the shell elements for the modes of (1, 3), (3, 2), (2, 4) and (4, 5). Circumferential mode shapes for $\alpha=20°$ are shown in Fig. 4.

The frequency comparisons between analytical solution developed here and finite element method are shown in Fig. 6. The discrepancy is defined as

$$\text{Discrerpancy } (\%) = \frac{\text{frequency by FEM-theoretical frequency}}{\text{frequency by FEM}} \times 100 \quad (15)$$

The largest discrepancy between the theoretical and finite element analysis results is 7.2% for the mode of (1, 2). Discrepancies defined by Eq. (15) are always less than 5% except for axial modes of $m'=1$, therefore the theoretical results agree well with finite element analysis results, verifying the validity of the analytical method developed. The compressibility of the fluid was found to reduce the natural frequency of the lower wet modes in the case of a fluid-filled cylindrical shell (Jeong and Kim, 1998). Therefore, discrepancies may be caused by the assumption that the water is incompressible in the theory.

The frequency variations of a conical shell with respect to the apex angle are shown in Fig. 6. Frequency comparisons for the various apex angles are shown in Fig. 7, which show that as the apex angle increases the frequencies tend to decrease. The rate of decreasing frequency has the same sinusoidal shape with respect to circumferential mode as shown in Fig. 8 except for $m'=1$. The effect are most severe for circumferential mode $n=3$ except for $m'=1$, where $n=1$ modes are most significantly affected.

The frequency variations of a conical shell without fluid with respect to the apex angle are shown in Fig. 9 and frequency comparisons for

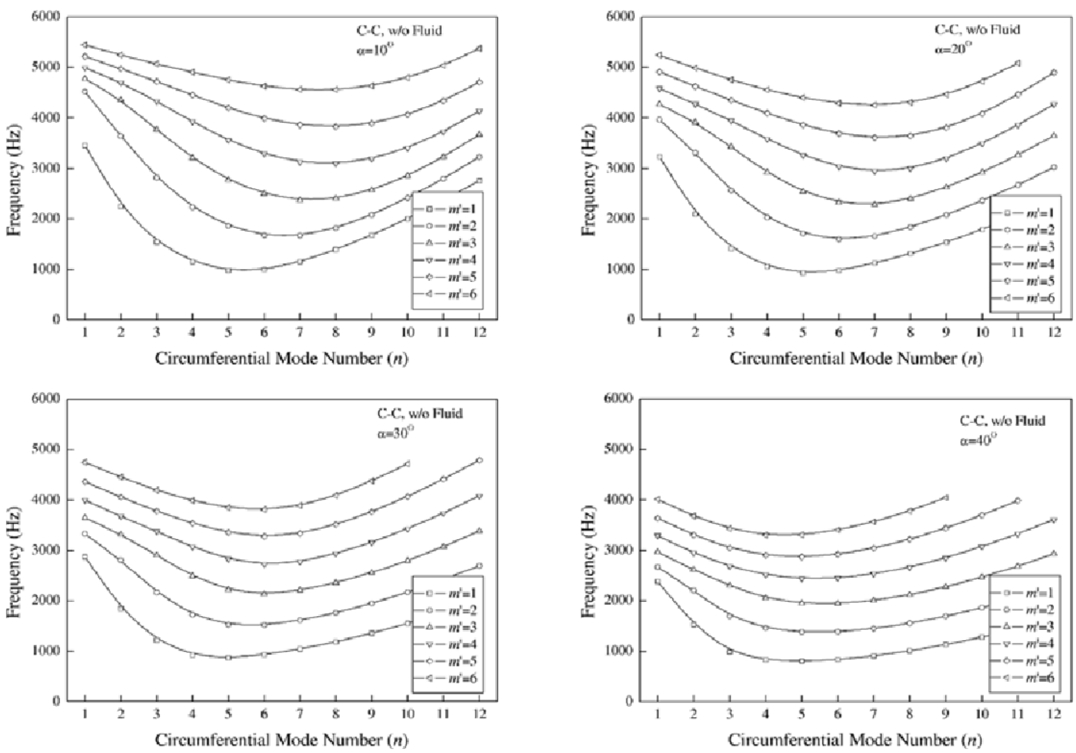

Fig. 9 Natural frequencies of a conical shell without fluid

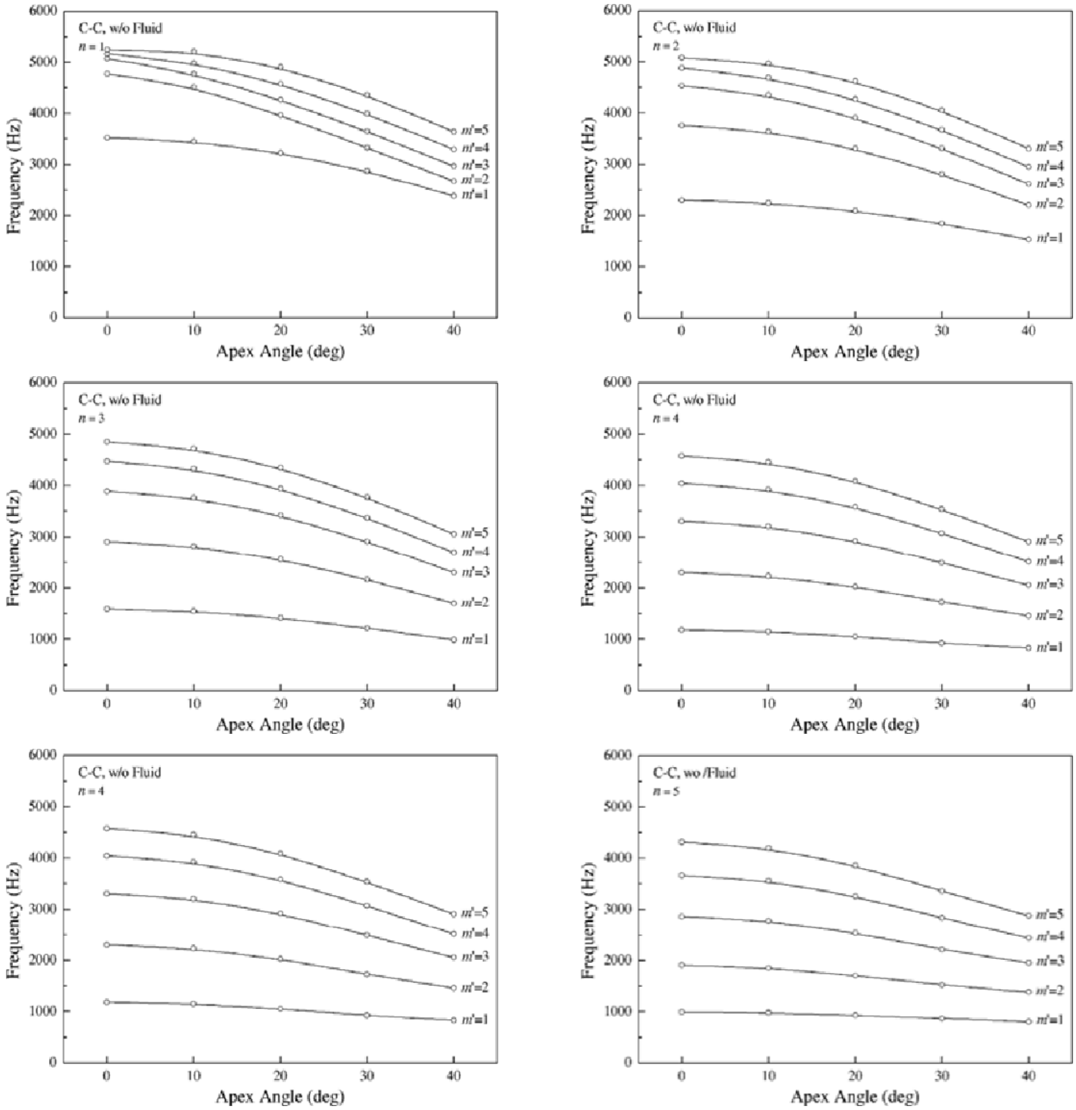

Fig. 10 Frequency comparisons of a conical shell without fluid

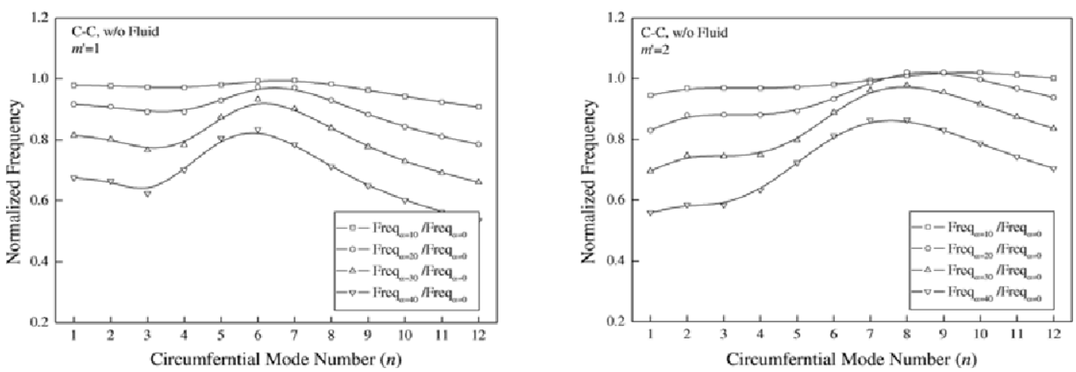

Fig. 11 Normalized frequencies of a conical shell w/o fluid to cylindrical shell

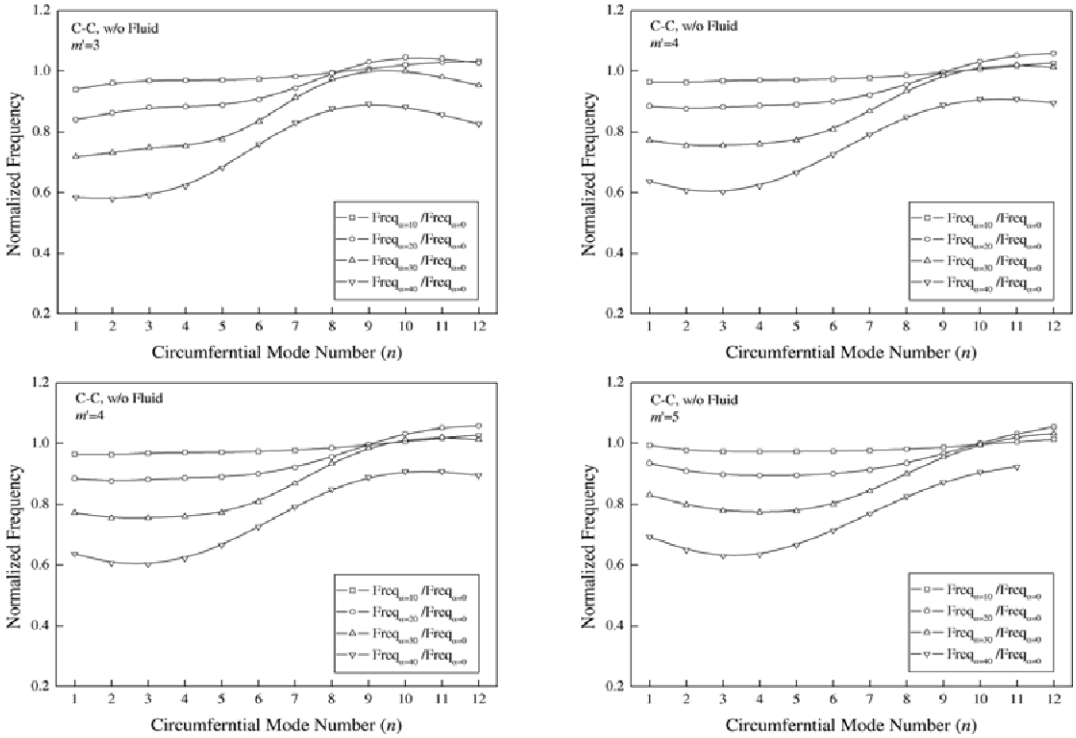

Fig. 11 Normalized frequencies of a conical shell w/o fluid to cylindrical shell (Cont'd)

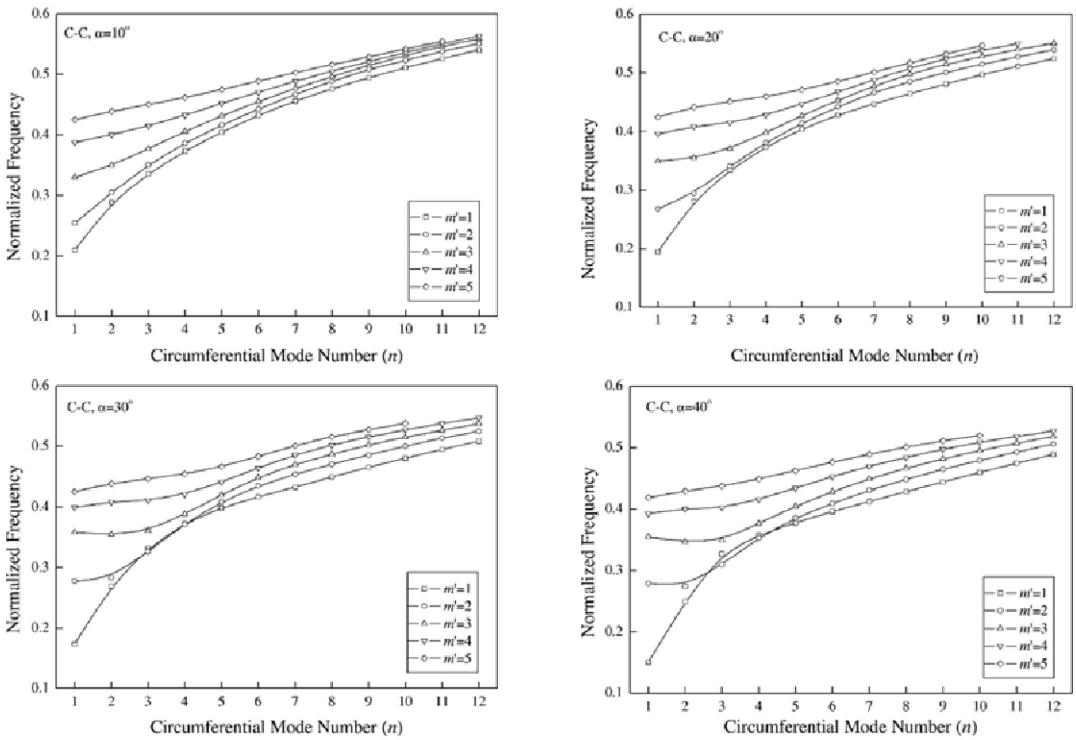

Fig. 12 Normalized frequencies of w/ fluid to w/o fluid

the various apex angles are shown in Fig. 10. In this case the effect of apex angle is a little different that of with-fluid case. For $m'=1,2$ and 3 the lowest circumferential mode $n=1$ are most influenced by the apex angle but $n=3$ modes for $m'=4$ and 5 are most affected as shown in Fig. 11 as in the case of with-fluid.

The effect of fluid filled on the frequencies can be assessed using the normalized frequency defined as the natural frequency of a structure with fluid divided by the corresponding natural frequency of the structure in air. The normalized natural frequencies have values between one and zero due to the added mass effect of fluid. Fig. 12 shows the normalized natural frequencies for various apex angles. As the apex angle increases, the reduction of frequencies due to the inclusion of fluid is more severe except for several modes such as (2,1), (3,1), (4,1), (3,2) and (4,2), where decreasing rate of frequencies increase. Also it is found that the normalized frequencies of with versus without fluid increase according to the increase of mode numbers, which means that lower circumferential and lower axial modes are more

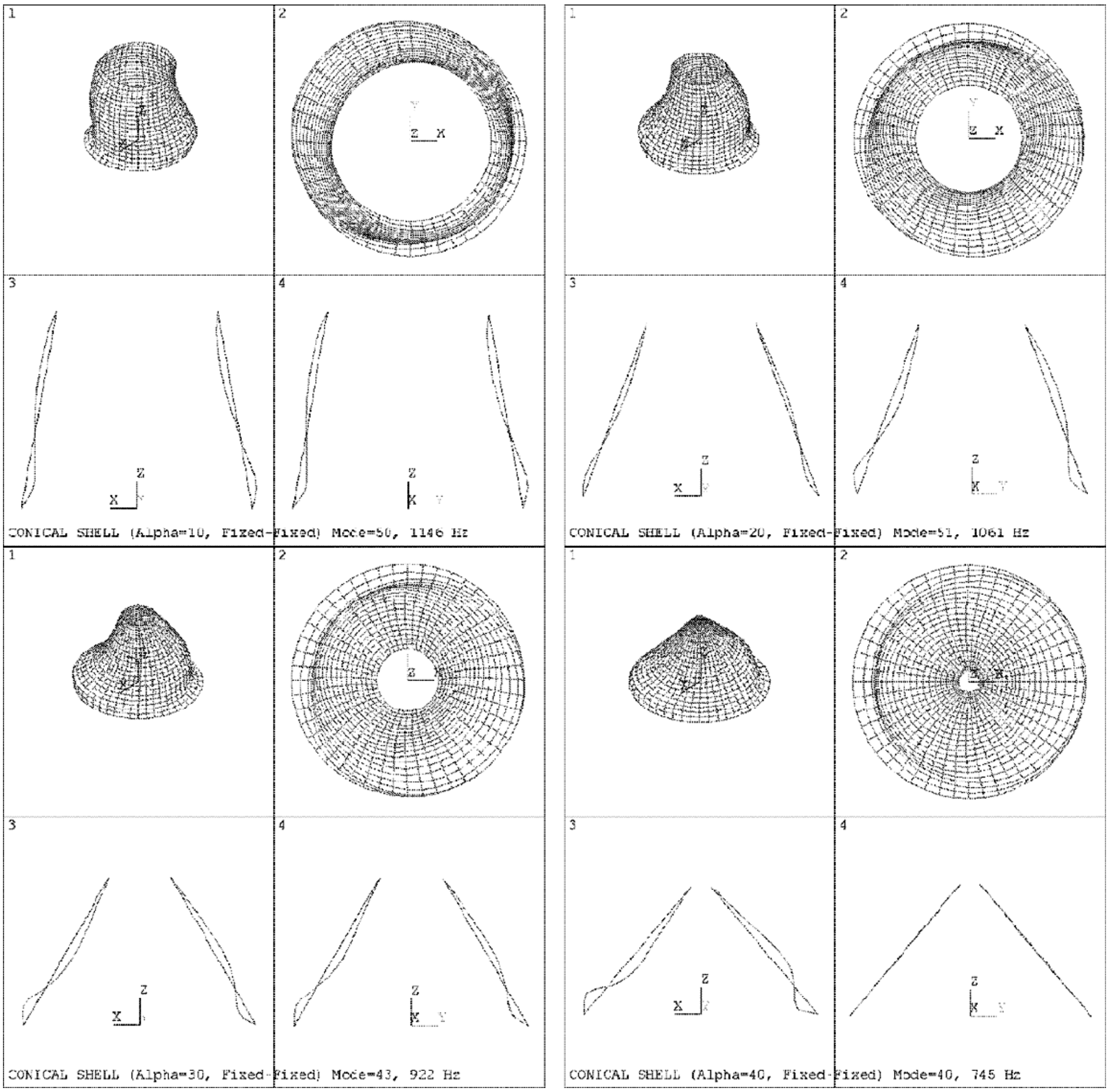

Fig. 13 Mode shapes of mode number (2, 1)

affected by the fluid. But (2, 1) mode larger than apex angle of 30° doesn't follow the general trend because it shows the combination of local modes as shown in Fig. 14, where the lower part of the shell moves more than the upper part. Generally, this kind of deviation from the general trend comes from the non-symmetric structure in the axial direction.

The vector plots of $m'=1$ representing the mode shape for the conical shell with apex angle of 40° are shown in Fig. 14. They show the maximum dynamic displacements of the water. Generally speaking, the liquid displacement near the shell is dominant and it gradually reduces as the liquid is far away from the shell. As the mode increases, the dynamic displacement of the water reduces

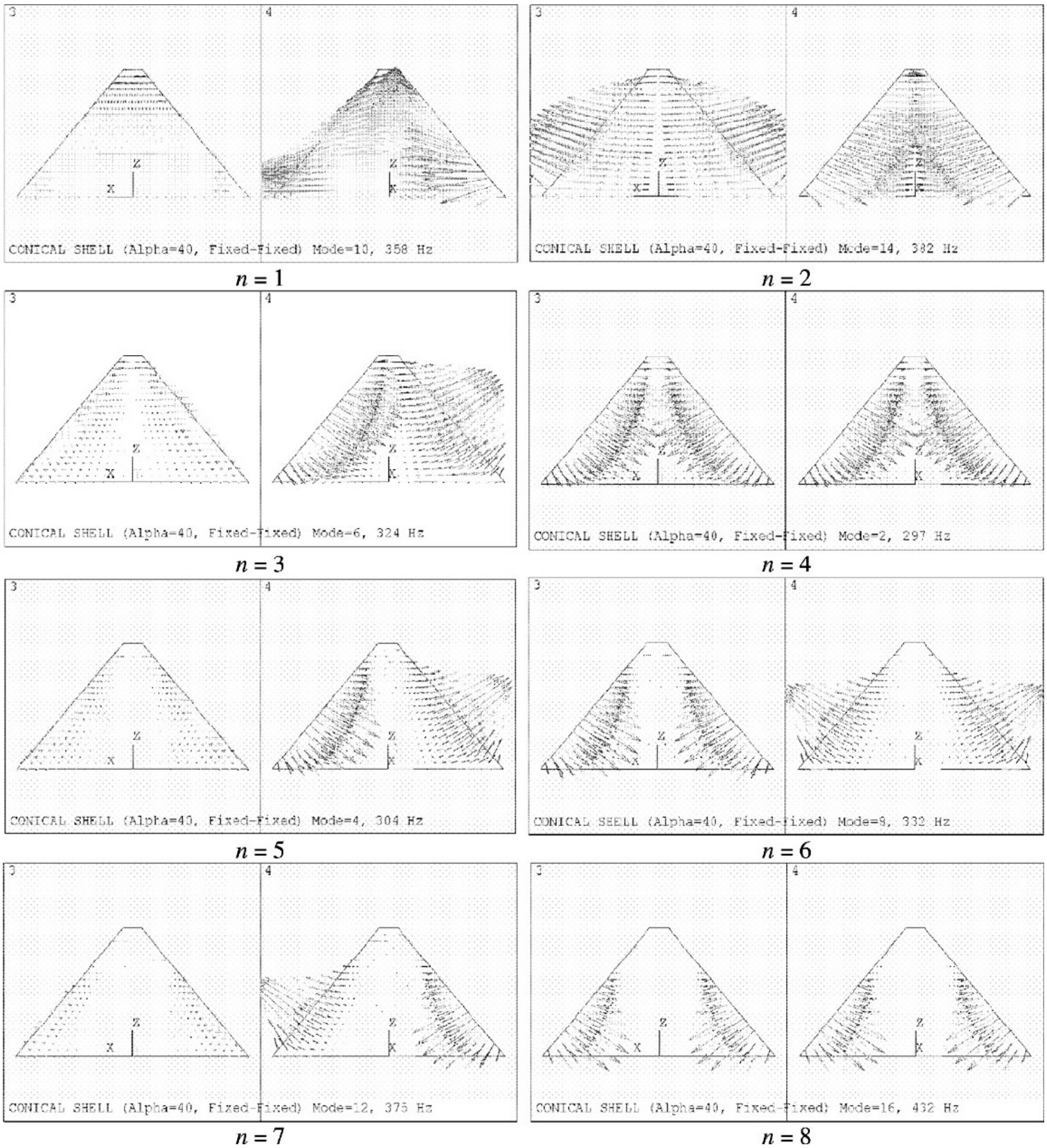

Fig. 14 Vector plot of mode shapes for $m'=1$

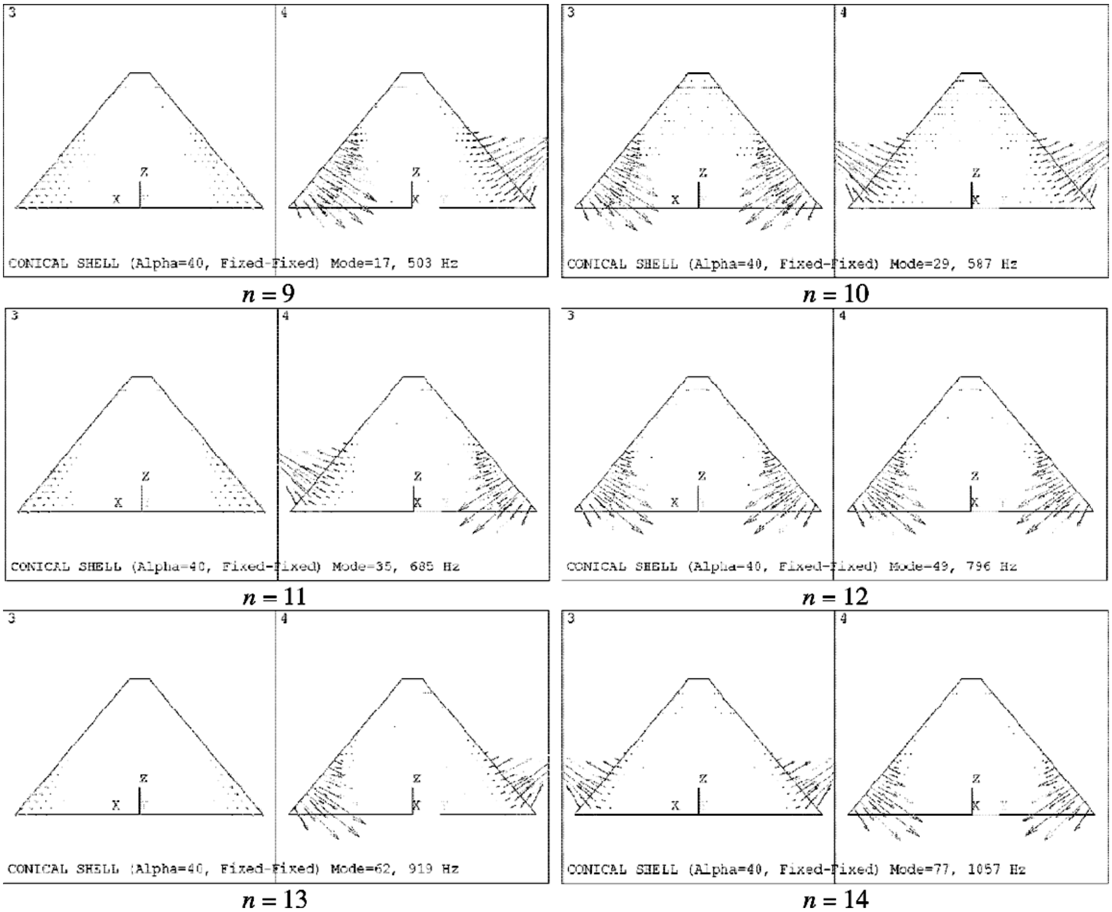

Fig. 14 Vector plot of mode shapes for $m'=1$ (Cont'd)

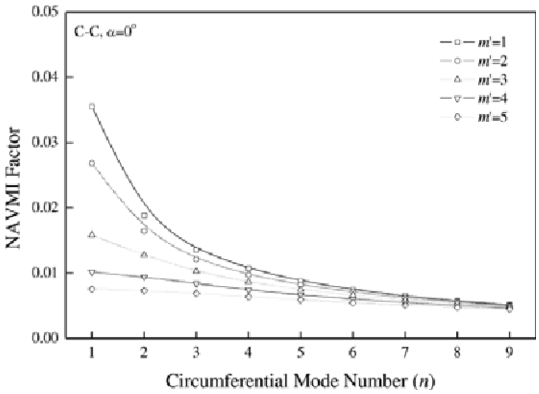

Fig. 15 NAVMI factors for $\alpha=0°$

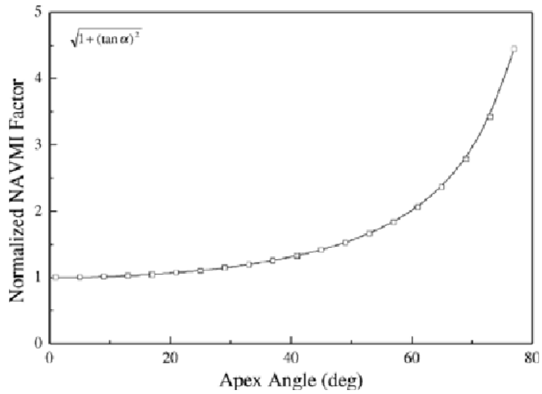

Fig. 16 Normalized NAVMI factor with respect to apex angle

resulting in the reduction of the fluid effect on the frequencies with the increasing number of modes, which is also shown in the normalized frequencies of the shell with fluid with respect to the shell without fluid as in Fig. 12.

Kwak and Kim (1991) introduced the non-dimensionalized added virtual mass incremental (NAVMI) factor to characterize the effect of fluid on the natural frequencies of circular plates in contact with fluid. The NAVMI factor Γ for the conical shell with fluid can be defined as

$$\Gamma=\frac{\rho_o}{\rho}\left[\left(\frac{\omega_{air}}{\omega_{water}}\right)^2-1\right]\left[\frac{2hR_o\sqrt{1+(\tan\alpha)^2}}{(R_o-h/2)^2}\right] \quad (16)$$

where ω_{air} and ω_{water} are the frequencies of the shell without and with water, respectively. For the apex angle of 0°, the NAVMI factor can be shown in Fig. 15 and it is clear that as the mode number increases the fluid effect decreases, which is concurrent with the result from the normalized frequencies of the shell with fluid with respect to without fluid. In addition, Eq. (16) indicates that the NAVMI factor is proportional to the apex angle by the ratio of $\sqrt{1+(\tan\alpha)^2}$, which relates the effect of the fluid on the frequencies to the apex angle of the conical shell as shown in Fig. 16. As the apex angle increases, the fluid effect increases, and therefore the frequencies decrease with the increasing apex angle as shown in Fig. 7.

5. Conclusions

An analytical method to estimate the coupled frequencies of the conical shells filled with fluid is developed using the velocity potential flow theory. To verify the validity of the analytical method developed, finite element method is used and the frequency comparisons between them are found to be in good agreement. The effect of fluid and the apex angle on the frequencies is investigated using a finite element method generating following conclusions ;

(1) As the apex angle increases the frequency decreases and for most axial modes the circumferential mode $n=3$ is most significantly affected by the apex angle.

(2) The inclusion of fluid affects the lower modes than the higher modes.

(3) The frequencies of the conical shells with fluid decrease to 0.15～0.55 of those of shells in air depending on the apex angle.

(4) The reduction rate of the frequencies due to the inclusions of the fluid increase with increasing apex angle except for several modes.

References

ANSYS, 2004, *ANSYS Structural Analysis Guide*, ANSYS, Inc., Houston.

Goldburg, J. E., Bogdanoff, J. L. and Marcus, L., 1960, "On the Calculation of the Axisymmetric Modes and Frequencies of Conical Shells," *The Journal of the Acoustical Society of America*, Vol. 32, pp. 738～7421.

Gupta, R. K. and Hutchinson, G. L., 1988, "Free Vibration Analysis of Liquid Storage Tanks," *Journal of Sound Vibration*, Vol. 122, pp. 491～506.

Han, R. P. S. and Liu, J. D., 1994, "Free Vibration Analysis of a Fluid-Loaded Variable Thickness Cylindrical Tank," *Journal of Sound and Vibration*, Vol. 176, pp. 235～253.

Jeong, K. H. and Kim, K. J., 1998, "Free Vibration of a Circular Cylindrical shell Filled with Bounded Compressible Fluid," *Journal of Sound and Vibration*, Vol. 217, pp. 197～221.

Jeong, K. H., Kim, K. S. and Park. K. B., 1997, "Natural Frequency Characteristics of a Cylindrical Tank Filled with Bounded Compressible Fluid," *Journal of the Computational Structural Engineering Institute of Korea*, Vol. 10, No. 4, pp. 291～302.

Kwak, M. K. and Kim, K. C., 1991, "Axisymmetric Vibration of Circular Plates in Contact with Fluid," *Journal of Sound and Vibration*, Vol. 146, pp. 381～389.

Leissa, A. W., 1973, *Vibration of shells*, NASA SP-288, National Aeronautics and Space Administration, Washington, D. C.

Mazuch, T., Horacek, J., Trnka, J. and Vesely, J., 1996, "Natural Modes and Frequencies of a Thin Clamped-Free Steel Cylindrical storage Tank Partially Filled with Water: FEM and Measurement," *Journal of Sound and Vibration*, Vol. 193, pp. 669～690.

Yamaki, N., Tani, J. and Yamaji, T., 1984, "Free Vibration of a Clamped-Clamped Circular Cylindrical Shell Partially Filled with Liquid," *Journal of Sound Vibration*, Vol. 94, pp. 531～550.